

Fermi National Accelerator Laboratory

FERMILAB-Conf-93/403-E

E761

Hyperon Weak Radiative Decays and Magnetic Moments

Peter S. Cooper
The E761 Collaboration

*Fermi National Accelerator Laboratory
P.O. Box 500, Batavia, Illinois 60510*

December 23, 1993

Submitted to the Proceedings of the *U.S. Japan Seminar on Hyperon Nucleon Interactions*,
Maui, Hawaii, October 25-28, 1993

Disclaimer

This report was prepared as an account of work sponsored by an agency of the United States Government. Neither the United States Government nor any agency thereof, nor any of their employees, makes any warranty, express or implied, or assumes any legal liability or responsibility for the accuracy, completeness, or usefulness of any information, apparatus, product, or process disclosed, or represents that its use would not infringe privately owned rights. Reference herein to any specific commercial product, process, or service by trade name, trademark, manufacturer, or otherwise, does not necessarily constitute or imply its endorsement, recommendation, or favoring by the United States Government or any agency thereof. The views and opinions of authors expressed herein do not necessarily state or reflect those of the United States Government or any agency thereof.

Hyperon Weak Radiative Decays and Magnetic Moments

Peter S. Cooper
(E761 Collaboration)

Fermi National Accelerator Laboratory, Batavia, IL 60510

ABSTRACT

We have measured the branching ratio and asymmetry parameter in the hyperon radiative decays $\Sigma^+ \rightarrow p\gamma$ and $\Xi^- \rightarrow \Sigma^-\gamma$ with samples of 34754 ± 212 and 211 ± 33 events respectively obtained in a polarized charged hyperon beam experiment at Fermilab. We have also set a new upper limit on the branching ratio for the radiative decay $\Omega^- \rightarrow \Xi^-\gamma$ and made a precision measurement of the magnetic moments of the Σ^+ and a first measurement of the magnetic moment of the anti(Σ^+). These results and the techniques used in these measurements are discussed.

1. Introduction

1.1 Hyperon Physics at Fermilab

Studies of hyperon production and decay properties have been an active part of the Fermilab physics program since the very beginning of the research program. Thirteen experiments have been completed in the past twenty years. The discovery of significant inclusive hyperon production polarization¹ has allowed whole classes of experiments which exploit these high energy polarized beams to measure rare hyperon decay asymmetry parameters and magnetic moments as well as the production polarizations themselves. The large fluxes and long hyperon lab decay lengths [~ 10 m] possible at Fermilab energies have permitted hyperon experiments to reach unprecedented levels of statistical precision.

1.2 E761

The experiment and results described here are from one of the last of these experiments. E761 was designed to make high statistics studies of the charged hyperon radiative decays. Magnetic moments and production polarizations were also measured. This paper summarizes many of the results²⁻¹⁰ from this experiment which has nearly completed it's analysis and publication phase.

2. Theory

2.1 Radiative Decays

Hyperon radiative decays represent a class of baryon decays which require contributions from both the weak and electromagnetic interactions. Hara proved¹¹ in 1964 that the asymmetries in radiative hyperon decay vanish in the SU_3 limit assuming only CP invariance and left handed currents in the weak interaction. Contrary to this prediction, the first measurements of the asymmetry parameter in the decay $\Sigma^+ \rightarrow p\gamma$ revealed some evidence for large negative asymmetries ($\alpha\gamma = -1.03^{+0.52}_{-0.42}$ ¹², -0.53 ± 0.36 ¹³). These were bubble chamber experiments where polarized Σ^+ were produced from the low energy $K^-p \rightarrow \Sigma^+\pi^-$ reaction. The average Σ^+ polarization was about 40%. A new measurement of the $\Sigma^+ \rightarrow p\gamma$ asymmetry was performed in 1987 at KEK in a counter experiment¹⁴ with Σ^+ produced in the reaction $\pi^+p \rightarrow \Sigma^+K^+$. The polarization of the Σ^+ was about 87%. From a sample of 190 events the asymmetry parameter was found to be -0.86 ± 0.13 (stat) ± 0.04 (syst). The summary of the world data on hyperon radiative decays prior to this experiment are shown in Table I.

TABLE I. Previous World Hyperon Radiative Decay Data^{15,18}

decay	branching ratio [$\times 10^{-3}$]	N	α parameter	N
$\Sigma^+ \rightarrow p\gamma$	1.25(7)	899	-0.83(12)	297
$\Xi^- \rightarrow \Sigma^-\gamma$	0.23(10)	9		
$\Xi^0 \rightarrow \Lambda\gamma$	1.06(16)	116	+0.43(44)	87
$\Xi^0 \rightarrow \Sigma^0\gamma$	3.56(43)	85	+0.20(32)	85
$\Lambda^0 \rightarrow n\gamma$	1.02(33)	24		
$\Omega^- \rightarrow \Xi^-\gamma$	<2.2(90%CL)			

The main difficulty in such experiments is separation of the $\Sigma^+ \rightarrow p\gamma$ radiative decay from the 400 times more abundant hadronic

decay $\Sigma^+ \rightarrow p\pi^0$. Moreover, the asymmetry parameter in the hadronic decay is large and negative ($\alpha_{\pi^0} = -0.980 \pm 0.016$)¹⁵ which raised the concern that the observed asymmetry in the $\Sigma^+ \rightarrow p\gamma$ decay might be, in fact, due to some contamination of the background into the $p\gamma$ sample. In addition, the number of $p\gamma$ events detected in these experiments was very small.

These observations raised a wide interest among theorists¹⁶. The classes of diagrams which contribute to these processes are shown in figure 1. The W exchange diagram can only contribute to radiative decays with a valence u quark in the initial state like $\Sigma^+ \rightarrow p\gamma$. Various models were investigated. None of these models could describe satisfactorily both the large negative asymmetry and the observed rate of the $\Sigma^+ \rightarrow p\gamma$ decay. This became possible only recently in the form of a QCD sum rule model¹⁷.

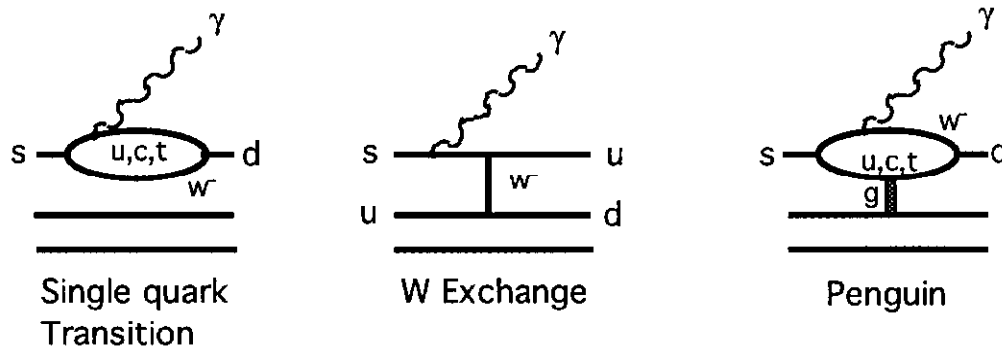


Figure 1. Quark Level Feynman diagrams for the processes contributing to hyperon radiative decays.

2.2 Hyperon Magnetic Moments

The magnetic moments of the members baryon octet provide a set of data with which to study the internal structure of the baryons. The simple SU_6 quark model¹⁹ describes these magnetic moments in terms of the magnetic moments of the three constituent quarks (u, d and s) and SU_6 wave functions. Many extensions to this simple idea have been suggested. None seem to improve the agreement with data beyond the $\sim 10\%$ level achieved with the simple model. The present world data (Table IV below) are much more precise than this. The particular issue which lead us to remeasure the Σ^+ moment

is that the previous two measurements^{20,21} are 1% measurements which disagree by 4%.

3. Experimental Methods

3.1 Fermilab Charged Hyperon Beam

This experiment was designed to perform a measurement of the asymmetry parameter in the $\Sigma^+ \rightarrow p\gamma$ decay on a high statistical level and with reliable separation from the $\Sigma^+ \rightarrow p\pi^0$ mode. The high energy hyperon beam at Fermilab provided a large flux ($\approx 2000/\text{sec}$) of Σ^+ with a polarization of 12%. The direction of the polarization was periodically reversed to allow the separation of the asymmetry from instrumental biases. To identify the $\Sigma^+ \rightarrow p\gamma$ decay we used charged particle spectrometers that provided high precision measurements of the missing neutral mass. In addition, a special photon spectrometer was constructed to determine the direction and energy of the photons.

The experiment was located in the Proton Center beam line at Fermilab. Protons of 800 GeV/c were steered and focused onto the hyperon production target. The targeting angle of the protons could be varied over the range ± 5 mrad. The charged hyperon beam originates from a one interaction length Cu target in the upstream end of a 7.3 m long hyperon magnet which imparts a transverse momentum (ΔP_t) of -7.5 GeV/c to the 375 GeV/c hyperon beam.

3.2 E761 Apparatus

The apparatus (figure 2) has four parts, the charged hyperon beam and three spectrometers; one each for the incident hyperon(Y), decay baryon(B) and photon in a generic hyperon radiative decay $Y \rightarrow B\gamma$.

The hyperon spectrometer consisted of 9 planes of 50 μm pitch silicon strip detectors (SSD) arranged in three stations and a 2m long magnet with a ΔP_t of +1.4 GeV/c. Hyperons are measured with resolutions (σ) of 0.7%, 12 μrad and 5 μrad in momentum, horizontal and vertical angles respectively. The baryon spectrometer includes 30 planes of multi wire proportional chambers (PWC) arranged in four stations. The first three stations have 8 planes each of 1 mm

pitch chambers in four views while the last station has 6 planes of 2 mm pitch chambers. The baryon spectrometer magnet consists of three 2 m long magnets operated in series with a combined ΔP_t of $-2.5 \text{ GeV}/c$. Baryons are measured with resolutions (σ) of 0.2%, 9 μrad and 6 μrad in momentum, horizontal and vertical angles respectively.

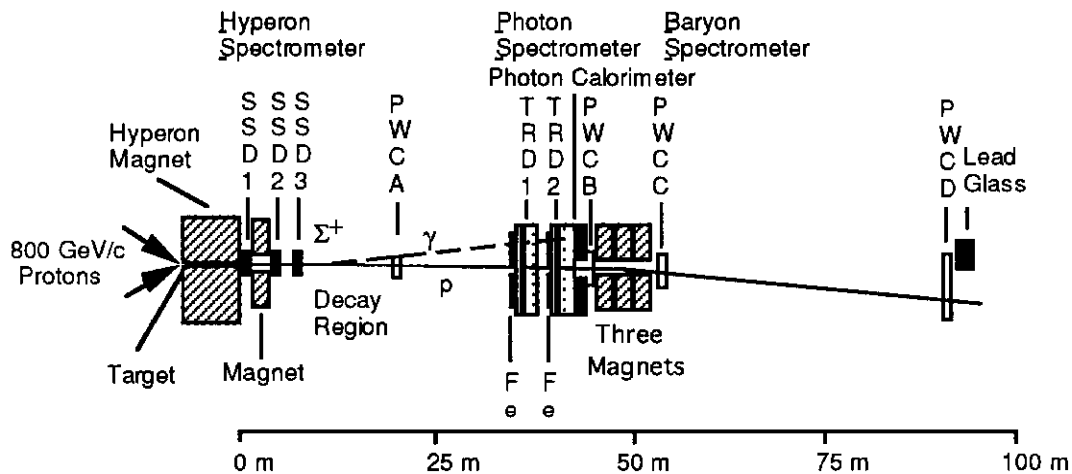


Figure 2. Plan view of the apparatus in the Fermilab Proton Center charged hyperon beam.

The photon spectrometer consisted of a set of tracking transition radiation detectors (TRD) to measure the position of the photon²² and a lead glass/bismuth germanate (BGO) photon calorimeter to measure the photon energy. Photons were converted in either of two 2.54 cm thick steel plates (≈ 1.5 radiation lengths each). Each plate is followed by 2 planes of PWC and 2 planes of TRD. The TRDs have a threshold of $\approx 2.5 \text{ GeV}/c$ for electrons and are sensitive to the high energy charged component of the photon shower. These electrons retain the initial direction of the photon to within the position resolution of the TRDs. The coordinate (X or Y) and fractional energy resolution (σ) of the photon spectrometer is 2 mm and $30\%/\sqrt{E(\text{Gev})} + 3\%$ constant term in quadrature respectively. There is a $76 \times 76 \text{ mm}^2$ hole in the photon spectrometer to allow the undecayed beam and the baryon through. This angular region is covered by a rear lead glass array. The hole in the front lead glass array is lined with BGO.

3.3 Rates and Data Taken

The trigger consisted of scintillation counters in each of the three spectrometers. A hyperon candidate was defined as the only particle within a 400 ns time window in the 100 kHz beam and a baryon by a single scintillator signal in a region where protons from Σ^+ decay were expected. A combination of scintillators in the photon spectrometer identified a converted neutral in one of the steel plates and >5 GeV was required in the photon calorimeter. No attempt was made at the trigger level to distinguish hadronic from radiative decays. The trigger rate was typically 0.8% of the beam rate and 24% of those triggers reconstructed as Σ^+ decays. The geometrical acceptance of the apparatus and trigger was 64% for radiative and 85% for hadronic decays.

During one month in the Fermilab 1990 fixed target running period 221×10^6 triggers were recorded on magnetic tape. These data were taken with complementary horizontal targeting angles near 3.7 mrad giving equal sub-samples with the Σ^+ polarization up and down. In the following two months 300×10^6 triggers were recorded with negative beam to provide samples of anti(Σ^+), Σ^- , Ξ^- and Ω^- decays. The apparatus for the negative beam running was modified by shortening the Baryon spectrometer and moving the photon spectrometer closer to the end of the decay volume. These changes were driven by the study of the $\Xi^- \rightarrow \Sigma^- \gamma$ decay mode where we magnetically analyzed the unstable Σ^- before it decayed. This required a baryon spectrometer whose length was comparable to the Σ^- lab decay length.

3.4 Analysis

Our asymmetry analysis does not depend upon the exact value of the polarization, only that it changes significantly between the two sub-samples. These data were first analyzed for hyperon and baryon tracks. In figure 3 is shown the distribution in the missing neutral mass squared $[M_{x^0}^2]$ for the hypothesis $\Sigma^+ \rightarrow p x^0$. This sample contains 48×10^6 hadronic, $\approx 67 \times 10^3$ radiative and $\approx 250 \times 10^3$ $K^+ \rightarrow \pi^+ \pi^0$ decays.

The photon spectrometer information is analyzed for 3.2×10^6 events in the range $-0.01 < M_{x^0}^2 [\text{GeV}^2/c^4] < 0.01$ which decayed in

the region from SSD3 to PWC A. The algorithm tests the hypothesis that the missing neutral is a single photon. At least 70% of the energy deposited in photon calorimeter is required to be within 5 cm of the extrapolated neutral track. Events consistent with the hypothesis $K^+ \rightarrow \pi^+ \pi^0$ or inconsistent with coming from the hyperon production target were also removed. A reduced TRD χ^2 is formed by summing the square of the error normalized distances between the extrapolated neutral track and the photon position determined by the TRDs.

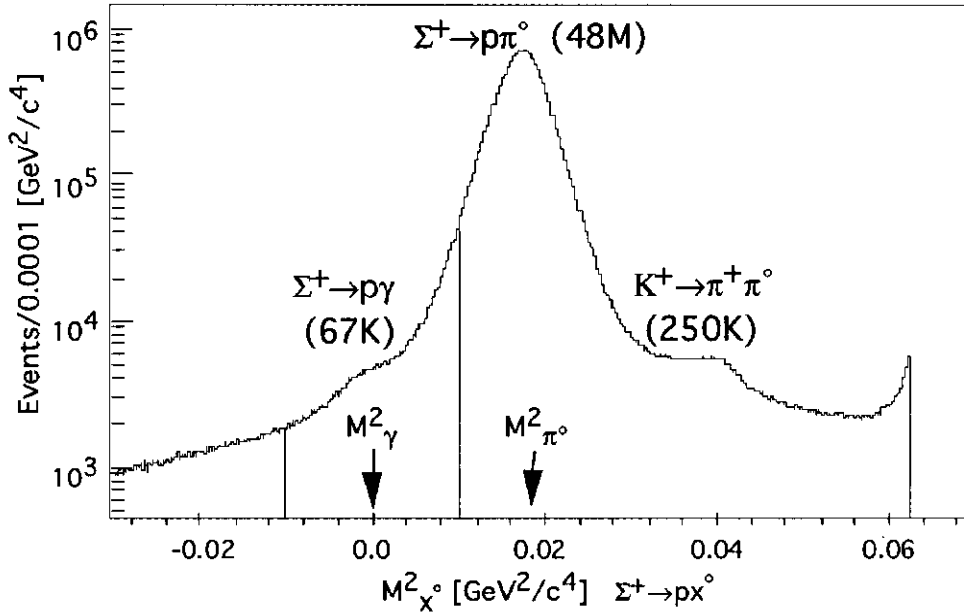


Figure 3. Event distribution of the mass squared of the missing neutral particle (X^0) for the hypothesis $\Sigma^+ \rightarrow pX^0$ for all candidates. The radiative decay region is shown.

The event distributions of $M^2_{X^0}$ for two TRD χ^2 regions [<1.0 and >4.0] are shown in figure 4. There is a clear excess of events near the photon mass for the region TRD $\chi^2 < 1.0$. The events at large TRD χ^2 model well the hadronic background under the radiative decay events. Four regions are shown in figure 4; signal (S) and background (B) in the region $|M^2_{X^0}| < 0.004$ [GeV^2/c^4] and two corresponding normalization regions (N and T). The fraction and number of radiative decay events in the signal region are $f = 1 - N_B N_T / N_N N_S = 0.8315 \pm 0.0016$ and $f N_S = 34754 \pm 212$ events respectively where the N's are the number of events in the

corresponding regions. The sample defined by these cuts contains 52% of all radiative decay events and has a relatively small contribution from background (17%). The asymmetry of this background is measured by analyzing events in the background (B) region ($\text{TRD } \chi^2 > 4.0$).

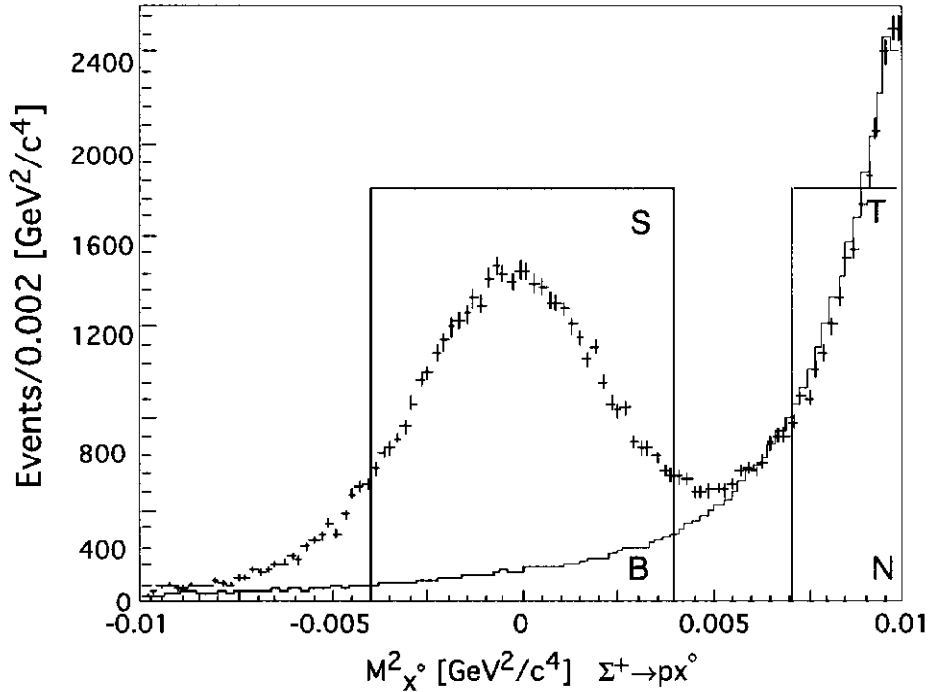


Figure 4. The missing mass squared distribution for all events with $\text{TRD } \chi^2 < 1.0$ (Signal, error bars) and $\text{TRD } \chi^2 > 4.0$ (Background, solid curve) normalized to equal area in the interval $[0.0072 < M^2_{X^0} < 0.01 \text{ (GeV}^2/\text{c}^4)]$ where the distribution is dominated by hadronic decays.

Analysis of the negative beam data proceeded in an analogous manner to that described above for the positive beam. The baryon momentum resolution is reduced to $\Delta P/P = 0.7\%$ by the shortened baryon spectrometer and an algorithm was developed to identify baryons which do not extrapolate to the end of the apparatus in order to distinguish $\text{anti}(\Sigma^+) \rightarrow \text{pbar } \gamma$ events from $\Xi^- \rightarrow \Sigma^- \gamma$ by requiring the baryon track to be consistent with the decay of the Σ^- .

4. Radiative Decay Results

4.1 $\Sigma^+ \rightarrow p\gamma$

In order to control systematic errors in the extraction of asymmetries it is necessary to control the differences in acceptance caused by changes in the beam phase space when the targeting angle is changed. This is done by dividing the data into bins in hyperon beam angle space, calculating the asymmetry for each bin and averaging those asymmetries to achieve a final result. The asymmetry $A_{ij} = \alpha_i P_j$ is the asymmetry parameter¹⁸ for the sample i times the polarization component in the direction j .

Table II. Asymmetry components for each sample. The quoted errors (shown in parenthesis) are statistical only. The Σ^+ polarization is in the Y direction so that A_X and A_Z should be zero.

Sample		A_X	A_Y	A_Z
Hadronic	π^0	-0.0050(21)	-0.1188(21)	-0.0011(21)
Signal	S	+0.0088(82)	-0.0884(83)	-0.0004(108)
Background	B	+0.0121(73)	-0.0938(81)	-0.0373(64)
Radiative	γ	+0.0082(100)	-0.0873(102)	+0.0070(130)

Applying the asymmetry analysis to the data samples in the signal and background regions of figure 4 produces the asymmetries shown in Table II. All the X and Z asymmetry components are consistent with zero with the exception of A_{BZ} . It is not surprising that there is a residual bias in this component; its correlation with the $A_{\gamma Y}$ is small and is included in the systematic error estimate. The asymmetries of the signal and background samples are nearly as large as the hadronic sample. The asymmetry of the radiative decay events is extracted by taking the asymmetry of the events in the signal region as a linear combination of radiative and background events with relative fraction f :

$$A_{S_Y} = f A_{\gamma Y} + (1-f) A_{B_Y} \quad (1)$$

The asymmetry parameter for the radiative decay is then determined from the ratio of radiative to hadronic asymmetries times the known value for the hadronic asymmetry parameter.

$$\alpha_\gamma = \frac{A_{\gamma\gamma}}{A_{\pi^0\gamma}} \alpha_{\pi^0} = \frac{\alpha_{\pi^0}}{f} \frac{1}{A_{\pi^0\gamma}} [A_{S\gamma} - (1-f) A_{B\gamma}] \quad (2)$$

The result² is $\alpha_\gamma = -0.720 \pm 0.086 \pm 0.045$ where the first error is statistical and the second systematic. This result is in agreement with the previous measurements. It confirms that the asymmetry in the Σ^+ radiative decay is indeed large and negative.

We have used a more refined analysis to measure the branching ratio for the $\Sigma^+ \rightarrow p\gamma$ mode. We obtain⁸ $[1.19 \pm 0.07 \pm 0.07] \times 10^{-3}$ where the first error is statistical and the second systematic. This result is also in agreement with the previous measurements. This confirms the hypothesis that the previous measurements did not overestimate the branching ratio by including hadronic background as signal.

In the negative beam data we have used exactly the same analysis to search for the decay $\text{anti}(\Sigma^+) \rightarrow \text{pbar} \gamma$. We observe about 400 events which give a preliminary branching ratio of $[1.42 \pm 0.20] \times 10^{-3}$ consistent with the $\Sigma^+ \rightarrow p\gamma$ result¹⁰.

4.2 $\Xi^- \rightarrow \Sigma^- \gamma$ and $\Omega^- \rightarrow \Xi^- \gamma$

The search for the $\Xi^- \rightarrow \Sigma^- \gamma$ decay is done with a technique similar to that used for $\Sigma^+ \rightarrow p\gamma$. The corresponding hadronic decay mode $\Xi^- \rightarrow \Sigma^- \pi^0$ is forbidden by energy conservation. The major background comes from $\text{anti}(\Sigma^+) \rightarrow \text{pbar} \pi^0$ events. These are separated from the Ξ^- radiative decays by the trick of requiring the baryon to decay. Figure 5 shows the missing neutral mass squared distribution for $\Xi^- \rightarrow \Sigma^- \gamma$ candidates and a Monte Carlo simulation of $\text{anti}(\Sigma^+) \rightarrow \text{pbar} \pi^0$ background events. A clear excess of 211 ± 33 events is observed at the photon mass. This corresponds to a branching ratio⁶ of $[1.22 \pm 0.23 \pm 0.06] \times 10^{-4}$ the first error is statistical and the second systematic. We have also measured the asymmetry parameter in this decay. Our result⁶, $\alpha_\gamma = +1.0 \pm 1.3$, makes it

marginally more likely that this parameter is positive. This is the best that can be done with the sample size we have.

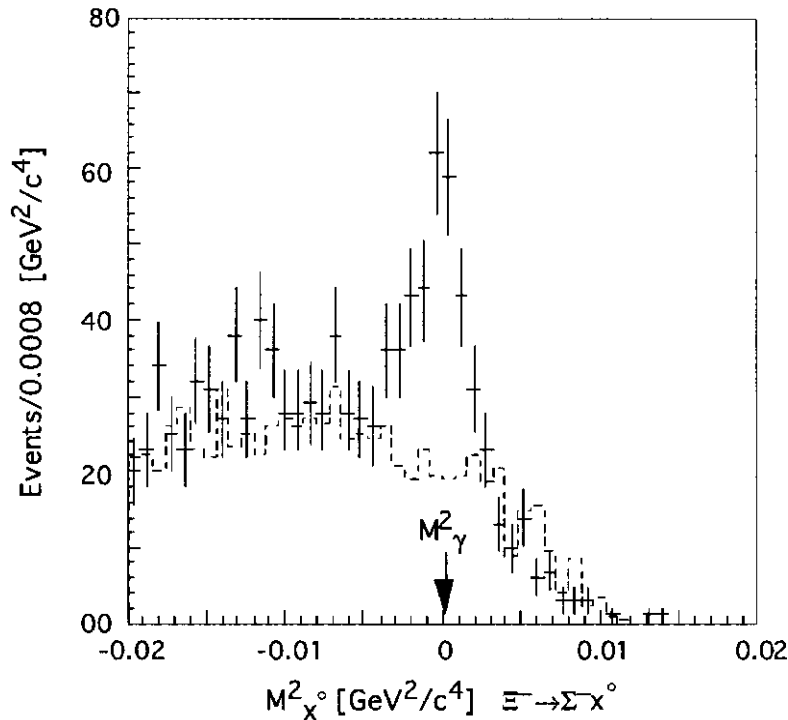


Figure 5. The missing mass squared distribution for the hypothesis $\Xi^- \rightarrow \Sigma^- x^0$. Dashed line is Monte Carlo events for the $\text{anti}(\Sigma^-) \rightarrow \text{pbar } \pi^0$ background.

We have also searched for the $\Omega^- \rightarrow \Xi^- \gamma$ radiative decay using similar techniques. We can set an improved branching ratio upper limit of 0.75×10^{-3} at 90%CL for this decay mode⁹.

4.3 Summary of Radiative Decay results

The summary of hyperon radiative decay results produced by E761 is shown in Table III. The E761 results confirm all the previous measurements. The $\Xi^- \rightarrow \Sigma^- \gamma$ branching ratio has dropped by a factor of two but is still in agreement with the previous result which was based upon 9 events. The asymmetry parameter in the $\Sigma^+ \rightarrow p \gamma$ decay is clearly large and negative. All questions of background contamination have been resolved. Hara's theorem is just wrong for this decay!

Table III. E761 Radiative Decay Results

decay	Parameter	PDG ^{15,18}	E761
$\Sigma^+ \rightarrow p \gamma$	Br [x10 ⁻³]	1.25 ± 0.07	1.19 ± 0.08 ⁸
	α_γ	-0.83 ± 0.12	-0.72 ± 0.10 ²
anti(Σ^+) pbar γ	Br [x10 ⁻³]	—————	1.42 ± 0.20 ¹⁰
$\Xi^- \rightarrow \Sigma^- \gamma$	Br [x10 ⁻³]	0.23 ± 0.10	0.122 ± 0.023 ⁶
	α_γ	—————	$+1.0 \pm 1.3$ ⁶
$\Omega^- \rightarrow \Xi^- \gamma$	Br [x10 ⁻³]	$<2.2(90\% \text{ CL})$	$<0.75(90\% \text{ CL})$ ⁹

5. Hyperon Magnetic Moment Results

5.1 Σ^+ and anti(Σ^+)

Based upon vertical targeting samples of $2.5 \times 10^5 \Sigma^+ \rightarrow p \pi^0$ events taken in positive beam and 1.2×10^4 anti(Σ^+) \rightarrow pbar π^0 events taken in negative beam we have measured the magnetic moments of the Σ^+ and anti(Σ^+) hyperons to be $+2.4613 \pm 0.0034 \pm 0.0040$ [NM] and $-2.428 \pm 0.0364 \pm 0.007$ [NM] respectively where the first error is statistical and the second systematic⁵. These results are consistent with the requirements of CPT invariance that a particle and anti-particle have magnetic moments equal in magnitude and opposite in sign. This measurement resolves the discrepancy between the previous two measurements and improves the precision to 0.2% making it the most precise hyperon magnetic moment measurement.

5.2 Summary of Hyperon Magnetic Moment results

The summary of hyperon magnetic moment results and a typical fit to the SU₆ quark model are shown in Table IV. The fit is done by using the proton, neutron and Λ^0 moments to fix the moments of the three quarks. The moments of the other hyperons are then determined by the model. This model reproduces the measurements to the 10% level one would expect from an SU₆ based model. The deviations from this simple description are measured

very well. No further experimental work will significantly change this situation. An improved theory is clearly required.

TABLE IV. Hyperon Magnetic Moments [NM]

Hyperon	Moment ^{5,15}	Quark Model	Diff
p	+2.792847	fixed	---
n	-1.913043	fixed	---
Λ°	-0.613(04)	fixed	---
Σ^{+}	+2.461(05)	+2.67	-0.207(05)
$\Sigma^{\circ} \rightarrow \Lambda^{\circ}$	-1.610(80)	-1.63	+0.020(80)
Σ^{-}	-1.160(25)	-1.09	-0.070(25)
Ξ°	-1.250(14)	-1.43	+0.177(14)
Ξ^{-}	-0.651(03)	-0.47	-0.161(03)
Ω^{-}	-1.940(220)	-1.84	-0.100(220)

6. Conclusions

In understanding both the radiative decay parameters and magnetic moments of the hyperons we now find ourselves in similar positions. The experimental results are precise and consistent. The theoretical situation seems to be static with little significant progress to report. The important Feynman diagrams at the quark level are well known for these processes. The problem seems to be in the understanding and inclusion of the hadronic structure of the baryons into the calculations. It is time for someone to build us a better baryon.

7. Acknowledgments

The author gratefully acknowledges the work of six former and two present graduate students who have produced much of the physics reported here. The errors in this manuscript are the sole property of the author.

We wish to thank the staffs of Fermilab and the St. Petersburg Nuclear Physics Institute for their assistance. The loan of the photon calorimeter lead glass from Rutgers University is gratefully acknowledged. This work is supported in part by the U.S. Department of Energy under contracts DE-AC02-80ER10587, DE-AC02-76CH03000, DE-AC02-76ER03075, DE-FG02-91ER40664, DE-FG02-91ER40682, DE-FG02-91ER40631, and the Russian Academy of Sciences.

References

- 1 G. Bunce, et.al., *Phys.Rev. Lett.* **36**, (1976) 1113.
- 2 M. Foucher, et.al., *Phys.Rev.Lett.* **68**,(1992) 3004 .
- 3 D. Chen, et.al., *Phys.Rev. Lett.* **69**, (1992) 3286.
- 4 A. Morelos, et.al., *Phys.Rev. Lett.* **71**, (1993) 2172.
- 5 A. Morelos, et.al., *Phys.Rev. Lett.* **71**, (1993) 3417 .
- 6 T. Dubbs, et.al., Submitted to *Phys.Rev. Lett.*
- 7 A. Morelos, et.al., Submitted to *Phys.Rev. Lett.*
- 8 S. Timm, et.al., To be Submitted to *Phys.Rev. D.*
- 9 I. Albuquerque, et.al., To be Submitted to *Phys.Rev. D.*
- 10 R. Mahon, et.al., To be Published.
- 11 Y. Hara, *Phys. Rev. Lett.* **12**, (1964) 378.
- 12 L.K. Gershin, et.al., *Phys. Rev.* **188**, (1969) 2077.
- 13 A. Manz, et.al., *Phys. Letters* **96B**, (1980) 217.
- 14 M. Kobayashi, et.al., *Phys. Rev. Lett.* **59**, (1987) 868 .
- 15 Particle Data Group, *Phys. Rev. D.* **45** II, (1992).
- 16 N. Vasanti *Phys. Rev. D* **13**, 1889 (1976), F.J. Gilman and M.B. Wise, *Phys. Rev. D.* **19**, (1979) 976, Y.I. Kogan and M.A. Shiftman, *Sov. J.Nucl. Phys.* **38**, (1983) 628, M.D. Scadron and M. Visinescu, *Phys. Rev.D.* **28**, (1983) 1117, M.K. Gaillard, X.Q. Li and S. Rudaz, *Phys. Letters* **158B**, (1985) 158, D. Palle, *Phys. Rev. D.* **36**, (1987) 2863, C. Goldman and C.O. Escobar, *Phys. Rev. D.* **40**, (1989) 106, P. Zenczykowski, *Phys Rev ,D* **44** (1991) 1485.
- 17 I.I. Balitsky, V.M. Braun, A.V. Kolesnichenko, *Nucl. Phys. B.* **312**,(1989) 509.
- 18 The sign convention for the alpha parameters are those of the Particle Data Group, *Phys. Letters* **170B** , (1986)154; $\alpha_{\gamma}(\pi^0)$ is the asymmetry parameter of the decay proton in the final state $\Sigma^+ \rightarrow p\gamma(\pi^0)$.
- 19 A. De Rujula, H. Georgi and S.L. Glashow, *Phys.Rev. D.* **12**, (1975) 147.
- 20 C. Ankenbrandt, et.al., *Phys.Rev. Lett.* **32**, (1985) 1.
- 21 C. Wilkinson, et.al., *Phys.Rev. Lett.* **58**, (1987) 855.
- 22 V.T. Grachev, et.al., in *Proceedings of the Symposium on Particle Identification at High Luminosity Hardon Colliders*, edited by Treva J. Gourlay and Jorge G. Morfin (Fermi National Accelerator Laboratory, 1989), p. 415.